UJEAS

UNIZIK JOURNAL OF ENGINEERING AND APPLIED SCIENCES

UNIZIK Journal of Engineering and Applied Sciences 5(3), September (2025), 2782-2798
Journal homepage: https://journals.unizik.edu.ng/index.php/ujeas
PRINT ISSN: 2992-4383 || ONLINE ISSN: 2992-4391

Development and optimization of fluted pumpkin stems fiber using Taguchi's approach for Natural Fiber Reinforced Plastics Composite (NFRPC)

Christopher Chukwutoo Ihueze[1*], Ebisike Paschal Soroibe[2], Uchendu Onwurah[3]
Department of Industrial and Production Engineering, Faculty of Engineering Nnamdi Azikiwe University, Awka. Anambra State
[*]Corresponding Author's E-mail: ebisike4real_82@yahoo.com

Abstract; This research article investigated the development and characterization of Fluted Pumpkin stem fiber (FPSF) and the use of Taguchi's approach for optimization Natural Fiber Reinforced Plastics Composite (NFRPC). Emphasis was on the fiber development process, fiber extraction, surface treatment and fiber characterization. In this work, the tensile test experiment has been conducted using treated and untreated Telfairia occidentalis stem fiber and the results showed that the treated fiber has high tensile strength value of 124.2N/mm^2, as compared to untreated fiber with 42.1N/mm^2. Furthermore, design of experiment (DOE) technique was planned using Taguchi *L9* orthogonal array method to optimize the properties of new composite material. The analysis of variance (ANOVA) and signal-to-noise ratio (SNR) was performed to determine the optimal parameter levels and its statistical significance on each of the properties (Thermal conductivity, Tensile strength,). The results showed that all the chosen parameters have significant effects on the properties of new material.

Keywords: Taguchi's approach, Fluted Pumpkin stem fiber, Thermal conductivity, Tensile strength Telfairia occidentalis, Analysis of variance (ANOVA).

1. Introduction

The amount of agricultural wastes generated in the African region annually demonstrates the inadequacies of various African countries to follow global trend of recycling (Incarnato et al, 2003). Ogah et al, 2022, reported that large quantities of wastes produced in Nigeria are underutilized yearly. The burning of agro-wastes and the inappropriate disposal of wastes (such as open dumping) are some of the regular practices of waste disposal and management in Nigeria (Ogah et al, 2022). The growing ecological concern and governmental laws has lead to rise in the demand of the natural fibers as a substitute of synthetic fibers in the production of modern materials (Sanadi et al, 2001). Generally, materials developed from agro-wastes are considered as environment friendly and bio-degradable materials (Ogah et al, 2022). These materials are now becoming the centre of attraction because of the numerous advantages offered by them (Shibata rt al, 2003). Apart from providing a clean environment for production, these materials are also inexpensive which further increases the interest of the scientific and engineering community to explore the possibilities of using these materials in various engineering applications (Ihueze et al, 2022).

In this research study a new variant of natural fiber called Fluted Pumpkin Stem Fiber has been introduced, characterized and model for the development of Fluted Pumpkin stem fiber (FPSF) for Natural Fiber Reinforced Plastics (NFRP). The importance of understanding these fiber surface and micro-structures helps in designing and engineering a particular material product.

In recent times, the engineering applications of composites have increased tremendously because of the continuous advancement in the quality of composites produced. Polymer matrix composites are the most common advanced composites. They provide great strength and stiffness along with resistance to corrosion (Hemmasi, et al, 2013;

Chaharmahali et al, 2014). Mechanical properties of a polymer can be controlled by the incorporation of well-defined modifier particles in the polymer matrix. Reinforcement of polymers with particulates plays an important role in the improvement of the mechanical properties of high-performance materials.

The negative environmental impact as a result of non-biodegradability of carbon/glass fiber reinforced polyester composites is creating pressure for the substitution of high energy consumption materials for natural and sustainable ones (Sanadi et al. 2001; Shibata, et al, 2003). Compared to synthetic fibers, natural fibers and particulates have shown advantages in aspects such as flexibility and toughness. So, there is a growing worldwide interest in the use of these fibers and particulates.

2.1 Review of related literature

The use of agro-based materials/wastes in reinforcing polymers has recently attracted the attention of researchers because of their advantages over other established materials. Agro-based materials are environmentally friendly, fully biodegradable, abundantly available, renewable, cheap and have low density. Precisely, researches have been carried out on Polyester composites with several agro wastes as reinforcements. (Ihueze et al, 2017; Okafor et al, 2021).

The constant advancing of computer and computing science has made infrared spectroscopy techniques striding further: The availability of a dedicated computer, which is required for the FTIR instrumentation, has allowed the digitized spectra to be treated by sophisticated data processing techniques and increased the utility of the infrared spectra for qualitative and quantitative purposes (Agrawal and Shaikh, 2014). Cellulose, which acts as the reinforcing material in the cell wall, is the main constitute in natural fibers (Casper et al, 2004). The cellulose molecules are laid down in microfibrils in which there is extensive hydrogen bonding between cellulose chains, producing a strong crystalline structure (Oya and Johnson, 2001).

Fourier Transform Infrared spectroscopy (FTIR), is nowadays one of the most important analytical techniques available to scientists (Wortmann and Arns. 2016). One of the greatest advantages of the infrared spectroscopy is that virtually any sample in any state may be analyzed (Annette et al, 2007; Wortmann and Arns. 2016). For example, liquids, solutions, pastes, powders, films, fibers, gases and surfaces can all be examined with a judicious choice of sampling technique. While, X-ray diffraction analysis, is routinely used to generate high-resolution images of shapes of objects and to show spatial variations in chemical compositions: (1) acquiring elemental maps or spot chemical analyses, (2)discrimination of phases based on mean atomic number (commonly related to relative density) (Ogah et al, 2022; Oya and Johnson, 2001) The review by Annette et al, 2007, demonstrates the applicability of dispersion infrared spectroscopy for natural fibers studies Fourier transform infrared spectroscopy (FTIR) has facilitated many different IR sampling techniques, including attenuated total reflection and diffuses reflectance infrared Fourier transform (DRIFT) spectroscopy. It has dramatically improved the quality of infrared spectra and minimized the time required to obtain data.

Agrawal and Shaikh (2014), studies the Qualitative and Quantitative characterization of textile material by Fourier transform infra-red. International Journal of innovative research in science, engineering and technology. The mechanical properties of linear low-density polyethylene (LLDPE) reinforced with dodecyl amine-modified graphene was investigated by Kuila. Their study showed improvements in the storage moduli and thermal stability of the nanocomposites with increasing dodecyl amine-modified graphene content (Wortmann and Augustin, 2003). Chaudhary et al, (2018), Investigated the Quantitative fiber mixture analysis by scanning electron microscopy: Part VI: Possibility and limitations of the analysis of binary speciality fiber/wool blends in view of test method IWTO-58. Rout et al, (2001), Studied the Quantitative analysis of fiber mixture analysis by scanning electron microscopy: Part V: Analyzing pure fiber samples and samples with small admixtures according to test method IWTO-58.

(Owen et al, 2023), Studied the transverse and in-plane thermal conductivities for oriented and randomly oriented composites for several volume fractions of fibers in hemp fiber reinforced composites. It was found that the orientation of fibers has a noteworthy influence on thermal conductivity of composites (Liu et al, 2018) determined various thermal properties, namely, thermal conductivity, thermal diffusivity and specific heat of flax fiber–HDPE biocomposites around 170–200oC temperature range. The thermal conductivity, thermal diffusivity and specific heat found to be decrease with increased fiber content, however there is no appreciable change in thermal conductivity as well as thermal diffusivity in the specified temperate range. Conversely, the specific heat of flax fiber–HDPE composites steadily increased with temperature.

Obasi, (2015) estimated the thermal properties of jute-cotton, sisal-cotton and ramie-cotton hybrid fabric reinforced unsaturated polyester composites. The volume fractions of ramie, sisal and jute fibers in the fabrics were found to be 0.77, 0.69, and 0.64 respectively. The results showed that sisal-cotton hybrid polyester composites have thermal conductivity 0.213-0.25 W/m-k and specific heat of 1.065-1.236 J/cm3 ^{o}C; Jute-cotton hybrid polyester composites have thermal conductivity 0.10-0.237 W/m-k and specific heat of 0.869-1.017 J/cm^3 ^{o}C; Ramie-cotton hybrid polyester composites have thermal conductivity 0.19-0.22 W/m-k and specific heat of 0.839-0.894 J/cm3 ^{o}C.

2.0 Materials and methods

Fluted pumpkin stems of about seven to eight months old species of *Telfairiaoccidentalis* were harvested from farm garden, at lower Anambra / Imo river basin in Southeast Nigeria. *Telfairiaoccidentalis* is a tropical vine grown in West Africa as a leaf vegetable and for its edible seeds. Otherwise known as fluted gourd, fluted pumpkin stem, okporo-ugu, and ikong-ubong, in their native dialect. It belongs to *Cucurbitaceae*family and is an indigenous to Southern Nigeria. The fluted pumpkin stems were collected after used as an agricultural waste material near a market dump-site sources in Ehime Mbano council area, Imo State, Nigeria. The selection of the fluted pumpkin stems fiber depends on the desired properties, availability, cost, and compatibility with the matrix material. The collected fluted pumpkin stems were washed with water to remove impurities such as dirt, dust, leaves, barkand then cut between anti-nodes into nodes as in figure 3.1.

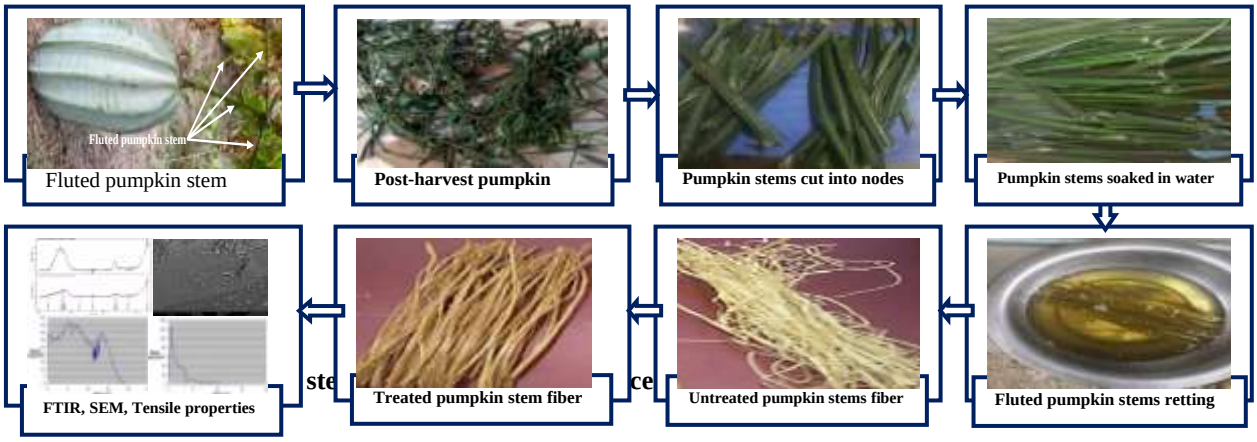

Figure 3.1: fluted pumpkin stems development and extraction process

3.2: Fluted Pumpkin Stem Fiber Extraction and Treatment Method

In this research study, the retting process involves the use of longitudinal section (NODES) of Fluted pumpkin stem between the ages of seven to eight months. Fluted pumpkin stem was sliced into small slabs (dimension) of about 10 to 20cm in length with slicer. The Fluted pumpkin stems were soaked in water for a period of 6 days. After which the fiber strands were soaked in separate concentrations of 2% and 3% mass over volume of sodium hydroxide (NaOH) respectively, for a minimum duration of twenty-four (24) hours and press with roller lesser, washed in diluted acetic acid solution to influence the cellulosic and non-cellulosic parts.

These steps as captured in figure 3.1 are intended to dissolve the cellulosic parts leaving lignin to float on top as a black substance. And finally, the fibers were rinsed and cleansed with distill water and dried under high sun intensity for 48 hours. Considering the high amount of lignin contains in Fluted pumpkin stem as compared with other natural stem fibers, chemical method or alkaline retting process was employed to extract the Fluted pumpkin stem fibers. This method helped to remove the amorphous regions of the Fluted pumpkin stem and also to reduce the lignin content of the elementary fiber.

3.3: Fiber Characterization

This research test experiment is in accordance with provisions of American Standard for Testing and Materials (ASTM). In this research study, tensile test experiment was conducted on the fluted pumpkin stem fiber using Universal materials testing machine (2500 KGF Capacity-Cat. PWG25W**,** M500 to 250T) at Turret Engineering Services Ltd, Port Harcourt, Rivers State, Nigeria. While Fourier Transform Infrared spectroscopy (FTIR) and Scanning electron microscope (SEM); was conducted at DICON Research and Development centre Kakuri, Kaduna State, Nigeria.

3.3.1Tensile Test experiment

The tensile tests on the fluted pumpkin stem fibers were performed using Universal Testing Machine. The samples were prepared according to ASTM D638 standard: Pretension 5.000N, width 1.000mm, thickness 1.000mm and sample length 250.000mm. The samples were placed in the grips of the universal testing machine and pulled at the test speed of 50.000 mm/min, until deformation occurred. The tensile strength and the tensile modulus of the treated and the untreated fluted pumpkin stem fibers were calculated using equations (31) and (3.2) respectively. (ASTM D1238-04 2004; ASTM D638-102010):

$$\text{Tensile Strength} = \frac{\mathrm{P}}{\mathrm{bh}} \tag{3.1}$$

$$Tensile\ Modulus = \frac{\sigma}{\varepsilon} \tag{3.2}$$

Where, P = Pulling force (N), b =Sample width (m), h = Sample thickness (m),σ =Stress (N/m^2), ε = Strain

Tables 3.2 to 3.3 and Figures 3.2 to 3.3 shows the stress-strain diagrams for the untreated and the treated fluted pumpkin stem fibers respectively. The tensile test results of the untreated fluted pumpkin stem fiber provide valuable insights into its mechanical properties and behavior. The untreated fiber exhibited a peak force of 42.1 N, elongating by 10.969 mm at the peak. This resulted in a stress at the peak of 42.1 N/mm² and a strain at the peak of 5.481%. The Young's modulus of the untreated fiber was calculated to be 21439.936 N/mm², indicating its stiffness. At the point of failure, the untreated fiber experienced a strain of 20.168% and a plastic strain of the same magnitude. The elongation at the break was 40.363 mm, and the strain after fracture was -0.068%. These values reflect the maximum deformation the untreated fiber underwent before breaking. The untreated fiber demonstrated a yield point at which it elongated by 0.53 mm. The corresponding yield force was 34.2 N, resulting in a stress at yield of 34.2 N/mm². The strain at yield was 0.265%, indicating the onset of permanent deformation. The untreated fiber showed an elongation of 1.96 mm at the point of fracture when subjected to a force of 0 N. This suggests that the untreated fiber experienced significant deformation before complete failure occurred. In terms of energy absorption, the untreated fiber absorbed 0.369 Nm of energy until reaching the peak force and 1.054 Nm of energy until failure. These values represent the untreated fiber's ability to withstand and dissipate energy during the test.

The results indicate that the treated fluted pumpkin stem fiber has a force of 124.2 N at the peak of the tensile test. At this point, the treated fiber elongated by 2.008 mm. The stress at the peak is also 124.2 N/mm^2, while the corresponding strain is 0.802%. The treated fiber experienced a strain of 14.846% at the point of fracture. The Young's modulus, which represents the stiffness of the treated fiber, is calculated to be 28219.82 N/mm^2. The width and thickness of the treated fiber specimens used in the test are 1 mm each. At the yield point, the treated fiber elongated by 1.96 mm. The elongation at the 0.000% proof stress level is 0.217 mm.

The treated fiber did not experience any force at the point of fracture (break), and the force at zero elongation is 5 N. The force at yield is 122.5 N, and the force at 0.000% elongation is 5 N. The stress at the 0.000% proof level is 28.349 N/mm^2.The plastic strain at the point of fracture is 14.846%, while the stress at yield is 122.5 N/mm^2. The strain at yield is 0.783%. The stress at zero elongation is 5 N/mm. The treated fiber elongated by 37.15 mm at the point of fracture, and the strain after fracture is -0.096%. The energy absorbed by the treated fiber until failure is 0.541 N.m. The elongation at the peak force is 2.008 mm, and the energy absorbed until the peak is 0.152 N.m. The strain at the upper yield point is 0.783%. The tensile properties of the treated fibers are by far greater than that of the untreated fibers. A great improvement on the tensile strength and the tensile modulus of the fluted pumpkin fiber was achieved as a result of chemical treatment. This is in line with previous studies (Ihueze et al, 2022; Ihueze et al, 2017).

Overall, the results indicate that the treated fluted pumpkin stem fiber exhibited considerable strength and ductility. It had a high peak force, suggesting good load-bearing capacity. The Young's modulus value suggests that the fiber possessed stiffness comparable to other materials commonly used in engineering applications. The fiber also demonstrated yield behavior, indicating its ability to withstand a certain amount of stress before permanent deformation occurs. The significant elongation at the point of fracture implies that the fiber can undergo substantial deformation before breaking. The energy absorption capabilities of the fiber indicate its potential for applications requiring impact resistance or energy dissipation. These properties make the treated fluted pumpkin stem fiber a promising material for various engineering applications, such as in lightweight structural components or as a reinforcement in composite materials.

Table 3.1 shows the comparison of the tensile properties of treated fluted pumpkin stem to that of other natural fibers. The tensile strength, tensile modulus and elongation at break of the fluted pumpkin stem fiber are comparable to those of other natural fibers that have used in reinforcement of composite materials. This shows that fluted pumpkin stem fiber is a good source of natural fiber that can be used in natural fiber reinforced polymer composites.

Table 3.1: Comparison of the Tensile Properties of Fluted Pumpkin Stem Fibers and Other Natural Plant Fibers

S/N	Fibers	T Strength (MPa)	Modulus of Elas (GPa)	Elongation at Break (mm)	Source
1	Fluted Pumpkin	124.2	28.22	2.008	The Present Study
2	Banana	10.854	1.63	6.085	Ihueze et al 2017
3	Bamboo cum	298	28.230	-	Kim et al,2010
4	Platain	170	62		Okafor et al, 2020
5	Raffia Palm	107.07	1.406	5.25	Hemmasi et al, 2013
6	Abaca	717	18.6		Shibata et al, 2003
7	Coconut	126.3	-	-	Ihueze &Achike, 2016
8	Zea mays root	13.243	0.5297	2.5	Mohanty et al, 2015

Table 3.2 **The tensile test result of fluted pumpkin stem treated fiber**

Test No	Force @ Peak (N)	Elong. @ Peak (mm)	Stress @ Peak (N/mm)	Strain @ Peak (%)	Strain @ Break (%)	Youngs Modulus (N/mm)	Width (mm)
1	124.2	2.008	124.2	0.802	14.846	28219.82	1.0

Test No	Thickness (mm)	Elong. @ Yield (mm)	Elong. @ 0.000 % Proof	Force @ Break (N)	Force @ 0.000 mm (N)	Force @ Yield (N)	Force @ 0.000 % (N)
1	1.0	1.96	0.217	0.0	5.0	122.5	5.0

Test No	Force @ Peak (N)	Plastic Strain @ Break (%)	Poisson's Ratio	Stress @ Yield (N/mm)	Percent Reduction of Area (%)	Strain @ Yield (%)	Secant Stiffness 0.000 to 0.000 % (N/mm)
1	124.2	14.846		122.5	0.0	0.783	

Test No	Stress @ 0.000 % Proof (N/mm)	Stress @ 0.000 mm (N/mm)	Stress @ Break (N/mm)	Elong. @ Break (mm)	Strain after Fracture (%)	Energy to Break (N.m)	Elong. @ Peak (mm)
	28.349	5.0	0.0	37.15	-0.096	0.541	2.008

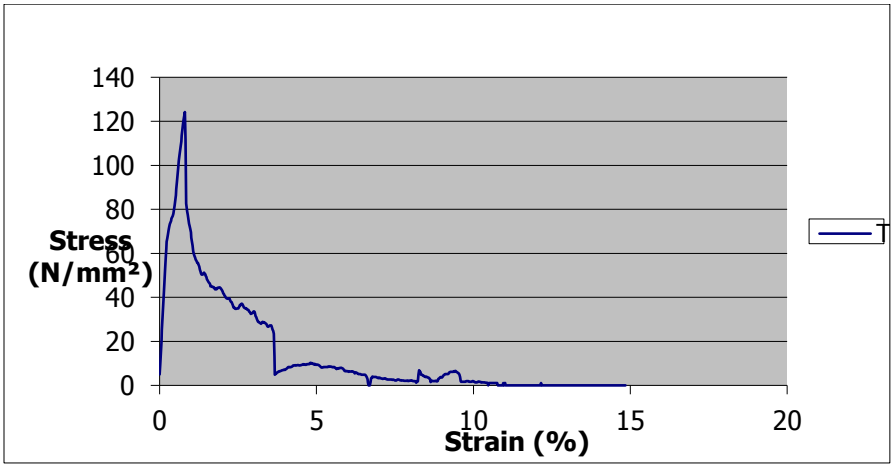

Figure 3.2: Tensile test result of treated fluted pumpkin stem fiber

Test No	Force @ Peak (N)	Elong. @ Peak (mm)	Stress @ Peak (N/mm²)	Strain @ Peak (%)	Strain @ Break (%)	Youngs Modulus (N/mm²)	Width (mm)
1	42.1	10.969	42.1	5.481	20.168	21439.936	1.0

Test No	Thickness (mm)	Elong. @ Yield (mm)	Elong. @ 0.000 % Proof (mm)	Force @ Break (N)	Force @ 0.000 mm (N)	Force @ Yield (N)	Force @ 0.000 % (N)
1	1.0	0.53	0.033	0.0	5.0	34.2	5.0

Test No	Force @ Peak (N)	Plastic Strain @ Break (%)	Poisson's Ratio	Stress @ Yield (N/mm²)	Percentage Reduction of Area (%)	Strain @ Yield (%)	Secant Stiffness 0.000 to 0.000 % (N/mm)
1	42.1	20.168		34.2	0.0	0.265	

Test No	Stress @ 0.000 % Proof (N/mm²)	Stress @ 0.000 mm (N/mm²)	Stress @ Break (N/mm²)	Elong. @ Break (mm)	Strain after Fracture (%)	Energy to Break (N.m)	Elong. @ Peak (mm)
	8.203	5.0	0.0	40.363	-0.068	1.054	10.969

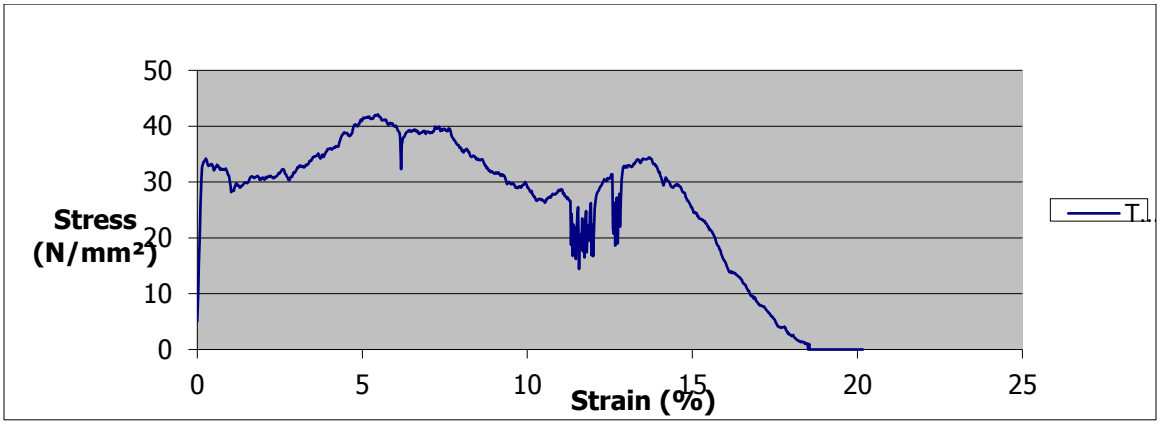

Figure 3.3: Tensile test result of un-treated fluted pumpkin stem fiber

3.4.2: Taguchi robust design

In Taguchi technique, the term "signal", represents desirable value (mean) and "noise" represents undesirable value (standard devia t ion) for the response (Raghunath and Pandy, 2016; Jiju Antony et al, 2016). Therefore, S/N ratio is the mean to standard deviation, which specifies the degree of predictable performance of a product or process in the existence of noise factors (Ihueze et al, 2012; Kamaruddin et al, 2018). (Jiju Antony et al, 2016).

Taguchi approach classifies objective functions into three categories, namely, smaller the better type, larger the better type and nominal the better type (Adeel Abbas et al, 2022; Ihueze et al, 2012). The optimum level for a factor

is the level, which results in highest S/N ratio value in the experimental space. The most widely used dispersion is the standard deviation (s) of the measured values. Using the set of n-values, the standard deviation is giving as in equation (3.3).

$$S= \frac{\sqrt{\sum_{i=1}^{n}(\frac{1}{y1})2}}{N-1} \quad (3.3)$$

The square of the standard deviation is called the variance (s^2) and is giving as in equation (3.4)

$$S^2 = \frac{\sqrt{\sum_{i=1}^{n}\frac{1}{(y1)}2}}{N} \quad (3.4)$$

The signal-to-noise ratio (S/N) is used in evaluating the quality of the product. It also measures the level of performance and the effect of noise factors on performance and is an evaluation of the stability of performance of an output characteristic. The Target values may be:

1. Smaller is better, choose when goal is to minimize the response. The S/N ratio can be calculated as given in Equation (3.5) for smaller the better

$$S/_N = -10\log\left(\frac{1}{n}\sum_{i=1}^{n} Yi^2\right) \quad (3.5)$$

2. Nominal is better: choose when goal is to target the response and it is required to base the S/N ratio on standard deviations only. The S/N ratio is calculated as given in Equation (3.6).

$$S/_N = -10\log\left(\frac{1}{n}\sum_{i=1}^{n}(Yi - Y0)^2\right) \quad (3.6)$$

3. The larger the better: Is the optimal level of the process parameters, is the level with the highest S/N ratio as in equation (3.7) (Raghunath and Pandey, 2017).

$$S/_N = -10\log\left(\frac{1}{n}\sum_{i=1}^{n}\frac{1}{(yi)}2\right) \quad (3.7)$$

Where yi is the performance response (measured value) and *n* is the number of experimental replications for each trial *i*.

The optimum response values of the properties are determined from the response table for means using equation 3.8 as derived by (Ji et al, 2021; Rohit, 2010), which is given as:

$$P_{opt} = G_{av} + (A_{opt} - G_{av}) + (B_{opt} - G_{av}) + (C_{opt} - G_{av}) + (D_{opt} - G_{av}) \quad (3.8)$$

Where P_{opt} = Optimum value for a response, G_{av} = average response value for the four factors considered, A, B, C, and D are the mean response for four factor parameters.

3.4.3: Analysis of Thermal conductivity using Taquchi's, L_9 Orthogonal array

Nominal-is-better, type category is used to evaluate the S/N ratio values for the thermal conductivity as stated in equation (3.6) using Minitab 19 software with due, to maximize the response S/N ratio values. The design formulation, experimental response and their statistical results were presented in table 3.5, while tables 3.6 and 3.7 presents the Response Table for Signal to Noise Ratios and Table for Means, Hence, the Main Effects Plot for Means and Main Effects Plot for SN ratio are presented in figures 3.8 and 3.9 respectively. Hence, Table 3.4 presents the Experimental Results for Thermal conductivity Obtained from the Sample.

Table 3.4: Experimental Results for Thermal conductivity Obtained from the Samples

EXP NO	T1(°C)	T2(°C)	∇T(K)	A(m^2)	Q(W)	K(W/mK)
1	40.0	35.8	277.35	0.2	300	0.11
2	40.0	36.0	277.15	0.2	300	0.11
3	40.0	35.2	277.95	0.2	300	0.12
4	40.0	35.8	277.35	0.2	300	0.11
5	40.0	35.1	278.05	0.2	300	0.12
6	40.0	36.1	270.05	0.2	300	0.12
7	40.0	35.5	277.65	0.2	300	0.11
8	40.0	35.8	277.35	0.2	300	0.11
9	40.0	35.1	278.05	0.2	300	0.12

Table 3.6 and Table 3.7 presents the Response Table for Signal to Noise Ratios and Table for mean of Means responses evaluated and their rankings for the thermal conductivity of fiber reinforced composites based on Nominal-is-better quality characteristics. The optimum responses values on this approach are obtained by sorting the delta values in an order of significantly affecting the thermal conductivity. From this analysis, it is observed that the factors that have the strongest influence were those with high rank of delta values. From the results in tables 3.6 and 3.7, it could be seen that the factors that have the strongest influence on the property were (C_3), (B_2), (A_2), (D_3) for S/N-ratio and (D_1), (B_3), (C_1) and (A_1) for mean of means in that order as depicts in Figure 3.8 and Figure 3.9 the Main Effects Plot for Means and Main Effects Plot for SN ratio respectively.

Table 3.5: Material Formulation and Experimental Response for Thermal conductivity, using fiber particle size of 50 Micrometer (μm)

Exp S/N	Parameters				Responses				Std. Dev.	SNR
	A	B	C	D	R_1	R_2	R_3	Mean, R		
1	50.76	25.38	12.69	6.52	0.11	0.13	0.14	0.126667	0.0152753	18.3735
2	50.76	26.04	13.02	8.86	0.11	0.12	0.13	0.120000	0.0100000	21.5836
3	50.76	26.74	13.35	11.16	0.12	0.12	0.13	0.123333	0.0057735	26.5928
4	52.08	25.38	13.02	11.16	0.11	0.11	0.11	0.110000	0.0000000	*
5	52.08	26.04	13.35	6.52	0.12	0.13	0.13	0.126667	0.0057735	26.8245
6	52.08	26.74	12.69	8.86	0.12	0.14	0.13	0.130000	0.0100000	22.2789
7	53.48	25.38	13.35	8.86	0.11	0.13	0.12	0.120000	0.0100000	21.5836
8	53.48	26.04	12.69	11.16	0.11	0.12	0.13	0.120000	0.0100000	21.5836
9	53.48	26.74	13.02	6.52	0.12	0.12	0.14	0.126667	0.0115470	20.8039

Table 3.6: The Mean of S/N-ratio Response for Thermal conductivity

LEVELS	A	B	C	D
1	40.36	38.16	38.77	39.95
2	42,39	41.59	39.38	40.00
3	39.58	41.17	43.18	42.39
Delta	2.80	3.43	4.41	2.44
Rank	3	2	1	4

Table 3.7: Response Table for Mean of Means

Levels	PVC (A)	$CaCO_3$ (B)	(C) DOP	FP Fiber(E)
1	0.1233	0.1189	0.1256	0.1267
2	0.1222	0.1222	0.1189	0.1233
3	0.1222	0.1267	0.1233	0.1178
Delta	0.0011	0.0078	0.0067	0.0089
Rank	4	2	3	1

3.4.4: Result Validation Using Analysis of Variance (ANOVA) for thermal conductivity

According to the ANOVA statistical results for thermal conductivity given in Tables 3.8, the p-values show that, all the parameters are statistically significant, implying that the parameters have significant impact on the property value because their p-values are less than 0.05. The results also show that the PVC with 57.00% contributions and $CaCo_3$ with 25.5% contribution have the highest influence on the thermal conductivity. These results are in good agreement with S/N ratio analysis.

Table 3.8: Analysis of Variance for SN Ratio thermal conductivity

Source	DF	Seq SS	Adj SS	Adj MS	F	%	P
PVC (A)	2	49.9658	49.9658	24.9829	10.20	57.0	0.012
$CaCO_3$ (B)	2	0.7685	0.7685	0.3842	8.50	25.5	0.010
DOP (C)	2	4.9363	4.9363	2.4682	3,90	7.00	0.000
FP Fiber(D)	2	7.9558	7.9558	3.9779	5.70	10.50	0.000
Residual Error	0	*	*	*	*	*	*
Total	8	63.6264				100.00	

S = 0.6486 R^2 = 92.2% R^2 (Adj) = 36.5%

Table 3.9: Analysis of Variance for Means of thermal conductivity

Source	DF	Seq SS	Adj SS	Adj MS	F	%	P
PVC (A)	2	0.048395	0.048395	0.024198	0.52	56.0	0.02
$CaCO_3$ (B)	2	0.091180	0.091180	0.045590	2.53	26.0	0.04
DOP (C)	2	0.012365	0.012365	0.006183	0.33	12.5	0.01
FP Fiber(D)	2	0.542291	0.542291	0.271146	0.142	6.50	0.04
Residual Error	0	*	*	*	*	*	*
Total	8	0.694232				100	

S = 0.6486 R^2 = 92.2% R^2 (Adj) = 36.5%

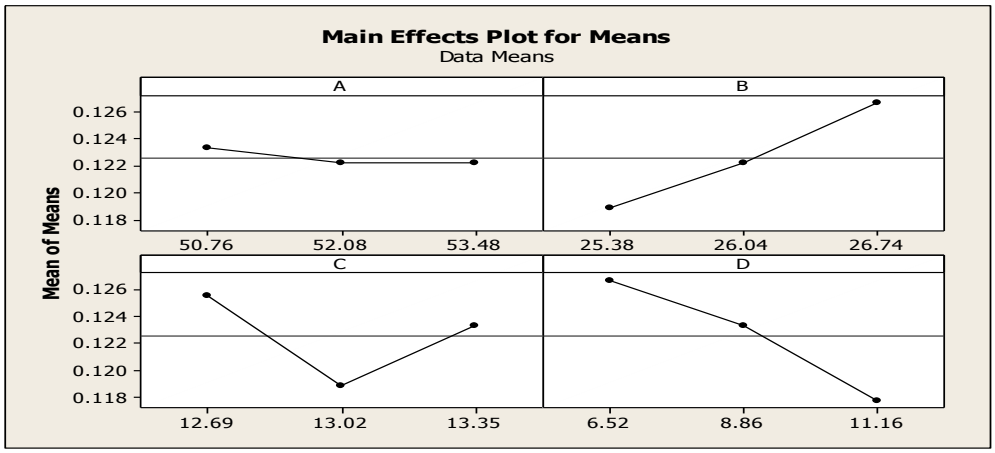

Figure 3.8: Depicts Main Effects Plot for Means

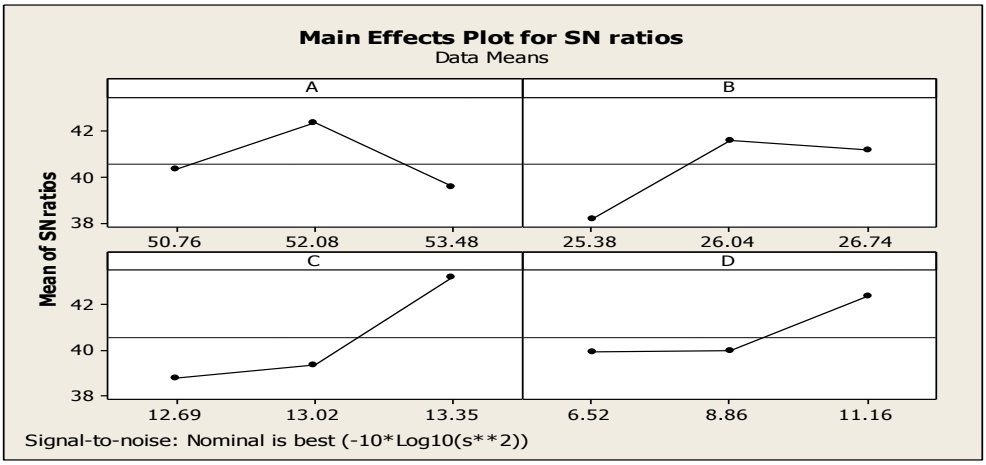

Figure 3.9: Depicts Main Effects Plot for S/N ratios

3.4.5: Determination of optimum response values for thermal conductivity: The expected responses were determine with the optimum parameter settings from the main effect plots and the values from the responses table for the signal-to-noise ratio and the response table for means (Okafor et al, 2013) using equation (3.8).

Using values in table 3.10, Response table for Mean of Means for fiber Particle Size of 50μm
G_{av}= 0.1256, $A_{opt} = A_1 = 0.1233$, $B_{opt} = B_3 = 0.1267$, $C_{opt} = C_1 = 0.1256$ and $D_{opt} = D_1 = 0.1267$
The optimum value is obtained as 0.1255 W/mK for mean and – 41.210 W/mK for signal-to-noise ratio against the predicated values in table 3.10 below:

Table 3.10: Optimum process parameter settings

Control Parameter/Factor		Optimum Level	Optimum Value
PVC	A	2	50.76
$CaCo_3$	B	2	25.38
DOP	C	3	13.02
FPS fiber	D	3	6.52

This result indicates that the selected control factor levels produced the best thermal conductivity. The difference between the predicted and the verified values is about 1.01% which means that predicted and verified values are very close to each others.

3.4.6: Verification Test

The purpose of the verification test was to confirm the validity of the predicted value. Minitab 19 software was utilized to predict the result of the process with the optimum settings that obtained by using S/N ratio.

Table 3.11: Depicts factor levels and Predicted values using Minitab 19

Parameters	Level	Value	Predicated value	
			Mean	SN ratio
PVC	3	50.76	0.133333	39.7506
CaCo3	2	26.04		
DOP	2	13.02		
Fiber particle	3	8.86		

3.4.7: Results analysis of Tensile strength using Taquchi's, L_9 Orthogonal Array

The S/N ratio larger-the-better category is used in evaluating the optimal response values for tensile strength in order to maximize S/N ratio response values as stated in equation (3.5). The design formulation, experimental response and their statistical results were presented in table 3.13, while Table 3.14 and Table 3.15 present the Response Table for Signal to Noise Ratios and Table for Means respectively using Minitab 19 software.

Table 3.12: Tensile test results obtained from the samples using fiber particle size of 50 Micrometer (μm)

Exp No	Force @ Peak (N)	Elong. @ Peak (mm)	Stress @ Peak (MPa)	Strain @ Peak (MPa)	Youngs Moduls (MPa)	Width (mm)	Thickns (mm)	Tensile strength (MPa)
1	950	12.10	15.20	0.0070	2171.4	35.00	2.00	13.57
2	900	10.00	9.04	0.0085	1063.3	35.00	2.00	12.85
3	1000	7.50	6.68	0.0045	1484.4	35.00	2.00	14.28
4	1000	12,30	6.85	0.0051	1343.3	35.00	2.00	14.28
5	850	10.55	12.17	0.0031	3925.8	35.00	2.00	12.14
6	900	9.50	7.40	0.0085	870.50	35.00	2.00	12.86
7	900	10.00	9.37	0.0044	2129.5	35.00	2.00	12.86
8	950	11.20	16.25	0.0054	3009.3	35.00	2.00	13.14
9	850	10.30	12.20	0.0085	1435.3	35.00	2.00	12.14

Table 3.13: Material Formulation and Experimental Response for Tensile strength, using fiber particle size of 50 Micrometer (μm)

Exp S/N	Parameters				Responses				Std. Dev.	SNR
	A	B	C	D	R_1	R_2	R_3	Mean, R		
1	50.76	25.38	12.69	6.52	13.57	14.00	13.45	13.6733	0.289194	22.7137
2	50.76	26.04	13.02	8.86	12.85	13.05	12.45	12.7833	0.305505	22.1279
3	50.76	26.74	13.35	11.16	14.28	14.55	14.70	14.5100	0.212838	23.2315
4	52.08	25.38	13.02	11.16	14.28	14.38	14.00	14.2200	0.196977	23.0563
5	52.08	26.04	13.35	6.52	12.14	12.77	13.00	12.6367	0.445234	22.0217
6	52.08	26.74	12.69	8.86	12.86	13.00	13.25	13.0367	0.197569	22.3013
7	53.48	25.38	13.35	8.86	12.86	13.25	12.30	12.8033	0.477528	22.1343
8	53.48	26.04	12.69	11.16	13.14	13.56	13.80	13.5000	0.334066	22.6013
9	53.48	26.74	13.02	6.52	12.14	12.68	12.72	12.5133	0.323934	21.9415

Table 3.14: The Mean of S/N-ratio Response for Tensile Strength

LEVELS	A	B	C	D
1	22.69	22.63	22.54	22.23
2	22.46	22.25	22.38	22.19
3	22.23	22.49	22.46	22.96
Delta	0.47	0.38	0.16	0.78
Rank	2	3	4	1

Table 3.15: Response Table for Mean of Means

Levels	PVC (A)	$CaCO_3$ (B)	DOP(C)	FP Fiber(D)
1	13.66	13.57	13.40	12.94
2	13.30	12.97	13.17	12.87
3	12.94	13.35	13.32	14.08
Delta	0.72	0.59	0.23	1.20
Rank	2	3	4	1

3.4.8: Experimental Result Discussion for Tensile Strength

For Tensile Strength the category of S/N Ratio used is the larger-the-better criteria. The optimum responses values on this approach were obtained by sorting the delta values in an order of significantly affecting the tensile Strength, from the analysis, it is observed that the factors that have the strongest influence were those with high range of delta values. The results in Table 3.14 and Table 3.15 shows that the factors that have the strongest influence on the property were (D_3), (A_1), (B_1), (C_1) for both S/N-ratio and means of mean in that order as depicts in Figures 3.10 and 3.11.

Table 3.16: Analysis of Variance for Tensile Strength S/N-ratio

Source	DF	Seq SS	Adj SS	Adj MS	F	%	P
PVC (A)	2	92.49	91.71	46.25	18.59	60.53	0.032
$CaCO_3$ (B)	2	16.70	15.92	8.35	21.41	20.51	0.010
DOP (C)	2	15.47	4.69	2.74	7.03	3.1	0.000
FP Fiber(D)	2	29.91	10.05	14.96	38.36	18.63	0.000
Residual Error	0	*	*	*	*	*	*
Total	8					100	

S = 18.4486 **R^2 = 90.6%** **R^2 (Adj) = 34.4%**

Table 3.17: Analysis of Variance for Means

Source	DF	Seq SS	Adj SS	Adj MS	F	%	P
PVC (A)	2	0.04131	0.041306	0.020653	12.25	42.0	0.02
$CaCO_3$ (B)	2	0.38993	0.389928	0.194964	11.97	35.5	0.03
DOP (C)	2	0.39600	0.396002	0.198001	5.57	18.25	0.03
FP Fiber(D)	2	0.35023	0.350232	0.175116	6.13	10.55	0.10
Residual Error	0	*	*	*	*	100	*
Total	8	1.17747					

S = 0.6486 **R^2 = 92.2%** **R^2 (Adj) = 36.5%**

3.4.8: Experimental Result Discussion for Tensile Strength:

Considering Tables 3.14 and 3.15, where the samples are produced using FPS fiber with particle size of 50μm, (D_3), (A_1), (B_1), (C_1) are the optimum response values for S/N-ratio and (D_3), (A_1), (B_1), (C_1) for means of mean in same order of parameters with the highest response values (strongest influence) and were chosen as could be seen in Figures 3.10 and 3.11

3.4.9: Result Validation Using Analysis of Variance (ANOVA) for Tensile Strength

The relative contribution percentage (%) and p-value of each factor obtained by the ANOVA method are given in Tables 3.16. It can be concluded, based on p-value that the significance of factors prevails in the following order of importance: (1) PVC (A); (2) $CaCO_3$ (B) and (3) DOP (C). The p-values show that, all the parameters are statistically significant, implying that the parameters have significant impact on the tensile strength value because their p-values are less than 0.05. The most significant factor is PVC (A); the percentage contribution of that parameter to tensile strength was 60.8%.

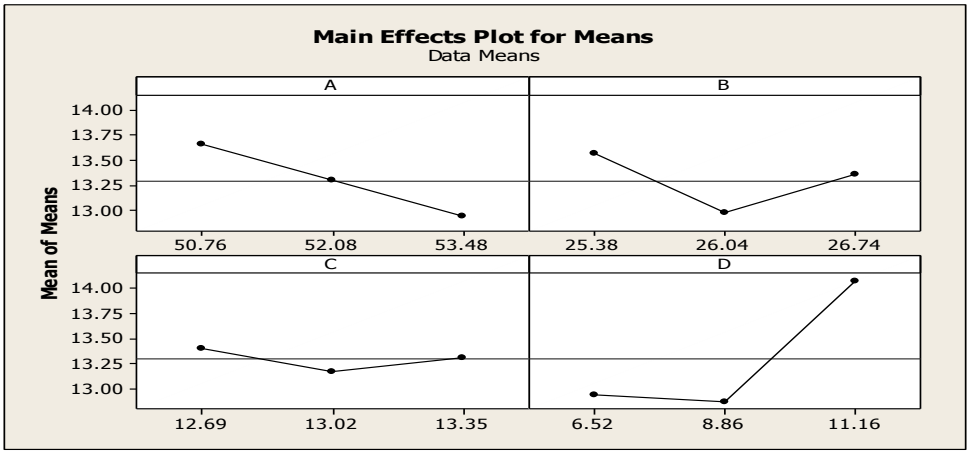

Figure 3.10: Depicts Main Effects Plot for Means

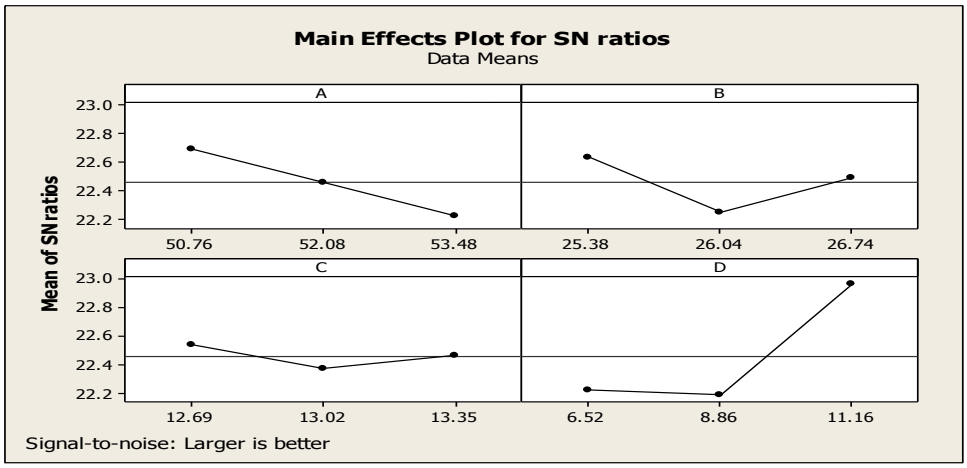

Figure 3.11: Depicts Main Effects Plot for S/N ratios

Figure 3.10 and Figure 3.11 depicts the main effects plot for means and main effects plot for SN ratio using larger-the-better of the tensile strength of the new composite material. The figure shows clearly the optimum values of the process parameter that will maximize the tensile strength of the new material. From figure 3.11, the optimum parameter settings are FPS fiber (D_3), PVC (A_1), $CaCo_3$ (B_1) DOP (C_3), and as expressed as: (A_1), (B_1), (C_1), (D_3) as shown in Table 3.18 below.

Table 3.18: Optimum process parameter settings

Control Parameter/Factor		Optimum Level	Optimum Value
PVC	A	1	50.76
$CaCO_3$	B	1	25.38
DOP	C	1	12.69
FPS Fiber	D	3	11.16

3.4.10: Determination of optimum response values for Tensile Strength: Using, equation (3.8), the optimum response values for Tensile Strength were obtained by direct substitution:

Using values in table 4.45, Response table for Mean of Means, fiber Particle Size of 150μm

G_{av} = 13.68, $A_{opt} = A_1$ = 13.66, $B_{opt} = B_1$ = 13.57, $C_{opt} = C_1$ = 13.40 and $D_{opt} = D_3$ = 14.08

The optimum value is obtained as 13.67 **MPa**

Table 3.19: Depicts factor levels and Predicted values using Minitab 19

Parameters	Level	Value	Predicated value	
			Mean	**SN ratio**
PVC	1	50.76	14.8089	23.4511
CaCo3	1	25.38		
DOP	1	12.69		
Fiber particle	3	11.16		

This result indicates that the selected control factor levels produced the best tensile strength. The difference between the predicted tensile strength and the verified tensile strength is about 1.01% which means that predicted and verified values are very close to each others.

4 Conclusions

This study focused on the development of Fluted Pumpkin Stem Fiber (FPSF) for Natural Fiber Reinforced Plastics (NFRP). The results obtained from this research indicate that fluted pumpkin stems can be effectively processed to extract fibers suitable for reinforcement in composite materials. The treatment process, involving retting and chemical treatments, helped to remove impurities and improve the compatibility of the fibers with the matrix material. The tensile tests demonstrated that the treated fluted pumpkin stem fibers exhibited higher strength, elongation, and stiffness compared to the untreated fibers. Chemical composition analysis using Fourier Transform Infrared (FTIR) spectroscopy provided insights into the molecular structure of the fibers. Xray diffraction analysis revealed the functional group and its weight fractions of the treated and untreated fluted pumpkin stem fibers. Overall, the findings of this research support the potential of fluted pumpkin stem fibers as reinforcements in Natural Fiber Reinforced Plastics (NFRP). The development of sustainable and eco-friendly composite materials using natural fibers like fluted pumpkin stems can contribute to reducing the reliance on synthetic materials and promoting environmental sustainability. Further research can focus on optimizing the processing techniques, exploring different fiber treatments, and investigating the performance of fluted pumpkin stem fibers in different composite formulations and applications.

Funding

The authors declare that no funds, grants, or other support were received during the preparation of this manuscript.

Competing Interests

The authors declare that they have no known competing financial interests or personal relationships that could have appeared to influence the work reported in this paper.

5 References

Agrawal SA, and Shaikh TN (2014) Qualitative and Quantitative characterization of textile material by Fourier transform infra-red. International Journal of innovative research in science, engineering and technology 3(1): 8496-8502.

Annette, N., Sudhakar, P., Ursula, K., Andrea, P. (2007). Fourier Transform Infrared Microscopy in Wood Analysis. In: Ursula Kües (Ed.) Wood production, wood technology, and biotechnological impacts. Universitätsverlag Göttingen. 179- ISBN 978-3-940344-11-3.

Casper C, Stephens JS, Tassi NG, Chase BD. (2004) Controlling surface morphology of electro spun polystyrene fibres: Effect of humidity and molecular weight in the electro spinning process. Macromolecules 37(2): 573-578.

Chaharmahali, M., Hamzeh, Y., Ebrahimi, G., Ashori, A., and Ghasemi, I. (2014). Effects of nano-graphene on the physico-mechanical properties of bagasse/polypropylene composites. *Polymer Bulletin*, *71*(2), 337-349.

Chaudhary, V., Bajpai, P. K., and Maheshwari, S. (2018). Studies on mechanical and morphological characterization of developed jute/hemp/flax reinforced hybrid composites for structural applications. *Journal of natural fibers*, *15*(1), 80-97.

Hemmasi, A. H., Ghasemi, I., Bazyar, B., & Samariha, A. (2013). Studying the effect of size of bagasse and nanoclay particles on mechanical properties and morphology of bagasse flour/recycled polyethylene composites. *BioResources*, *8*(3), 3791-3801.

Ihueze CC, Okafor CE, Onwurah UO, Obele CM, Obuka NSP, Abdulrahman J, Okoli NC, (2022). Integrity appraisal of long-term hydrostatic strength (LTHS) of plantain fibre reinforced HDPE (PFRHDPE) for pressure piping applications. Petroleum Technology Development12(1):47-61

Ihueze CC, Okafor CE, Onwurah UO, Obuka SN, Kingsley-omoyibo QA (2023). Modelling creep responses of plantain fibre reinforced HDPE (PFRHDPE) for elevated temperature applications. Advanced Industrial and Engineering Polymer Research. 6(1): 49-61. https://doi.org/10.1016/j.aiepr.2022.06.001

Ihueze CC, Oluleye AE, Okafor CE, Obele CM, Abdulrahman J, Obuka NS, Ajemba R (2017) Development of plantain fibres for application in design of oil and gas product systems. Petroleum Technology Development Journal: An International Journal 7(1):32-51.

Incarnato, L., Scarfato, P., Acierno, D., Milana, M. R., & Feliciani, R. (2003). Influence of recycling and contamination on structure and transport properties of polypropylene. *Journal of applied polymer science*, *89*(7), 1768-1778.

Liu JJ, Zou LN, Lv FB, An QB, Liu J, et al. (2015) Application of spectroscopy technology in textiles. International conference of Electrical, Automation and Mechanical Engineering, published by Atlantis Press pp. 482-484.

Ogah A.O, Ezeani O.E, James T.U(2022) Mechanical and morphological properties of fluted pumpkin stem fiber (Telfairaoccidentalis) recycled high density polyethylene nanocomposites. South Asian Res J Eng Tech 4(4):46-54.

Okafor CE (2021) Review of natural fiber composite design for sustainable infrastructural development. In:Anyogu FA, Eme CA, Ogbodo JA (ed) University-led knowledge and innovation for sustainable development,Nnamdi Azikiwe University Book Series on Sustainable Development, 1st ed.,Boldscholar Research Ltd, Abuja, pp. 82-98.

Okafor CE, Ihueze CC (2020)Strength analysis and variation of elastic properties in plantain fiber/polyester composites for structural applications.In: Tri-Dung Ngo (ed)Composite and nanocomposite materials - from knowledge to industrial applications, Intech Open, London,pp 1-23.

Okafor CE, Metu CS (2019) Theoretical fatigue response of plantain fiber based composites in structural applications. In: Zingoni A (ed)Advances in Engineering Materials, Structures and Systems: Innovations, Mechanics and Applications.Taylor & Francis Group, London,pp. 638 643. DOI: 10.1201/9780429426506-112

Owen MM, Achukwu EO, Romli AZ, MdAkil H (2023) Recent advances on improving the mechanical and thermal properties of kenaf fibers/engineering thermoplastic composites using novel coating techniques: A review. Composite Interfaces, 1-27.

Oya N, and Johnson D.J, , 2001 "Longitudinal Compressive Behavior And Microstructure Of PAN-Based Carbon Fibers," *Carbon*, vol. 39, pp. 635-645**.**

Rout J, Tripathy J,S, Nayak S.K, Misra M, and Mohanty A ,K, , 2001. "Scanning Electron Microscopy Study Of Chemically Modified Coir Fibers," *Journal of Applied Polymer Science*, vol. 79, pp. 1169-1177

Sanadi, A. R., Hunt, J. F., Caulfield, D. F., Kovacsvolgyi, G., & Destree, B. (2001). High fiber low-matrix composites: kenaf fiber/polypropylene, in: Proceedings of 6th International Conference on Wood Fiber-Plastic Composites, Madison WI, USA.

Shibata,M Ozawa K, Teramoto N, Yosomiya R, and Takeishi H, 2003. "Natural Composites Made From Short Abaca Fiber And Natural Degradable Polyesters," *Macromolecular Material Engineering*, vol. 208, pp. 35-43,

Wortmann FJ, and Augustin P (2003) Quantitative fiber mixture analysis by scanning electron microscopy: Part VI: Possibility and limitations of the analysis of binary speciality fiber/wool blends in view of test method IWTO-58. Textile Research Journal 73(9): 781-786.

Wortmann FJ, Arns W (2016) Quantitative fibre mixture analysis by scanning electron microscopy, Part I: Blends of mohair and cashmere with sheep's wool. Textile Research Journal 56(7): 442-446.